Journal of Electronic Research and Application, 2024, Volume 8, Issue 6
http://ojs.bbwpublisher.com/index.php/JERA
ISSN Online: 2208-3510
ISSN Print: 2208-3502

Real-Time Wind Speed Analysis at Wind-Damaged Tower of a Transmission Line

Jiehua Ding[1], Xiaoling Yang[2]*, Yongsheng Zhao[1]

[1]Central Southern China Electric Power Design Institute CO., LTD. of China Power Engineering Consulting Group, Wuhan 430068, Hubei Province, China
[2]School of Science Hubei University of Technology, Wuhan 430068, Hubei Province, China

***Corresponding author:** Xiaoling Yang, yangxiaoling@hbut.edu.cn

Abstract: Affected by the Super Typhoon "Mangkhut," a total of five base towers of a transmission line in the mountainous area of China collapsed. In this paper, a mathematical model is established based on the Shuttle Radar Topography Mission (SRTM) data near the accident tower. The measured wind speed in the plain area under the mountain is used as the calculation boundary condition. The wind speed at the top of the mountain is calculated by using a numerical simulation method. The design wind speed and calculated wind speed at the tower site are compared, and the influence of wind speed on tower position in this wind disaster accident is analyzed.

Keywords: Power transmission line; Wind disaster; Design wind speed; Real-time wind speed; Numerical simulation

Online publication: November 29, 2024

1. Introduction

At 20:00 on September 7, 2018, Typhoon Mangkhut formed in the northwest Pacific Ocean. On September 15, Typhoon Mangkhut made landfall in the northern Philippines. At 18:00 on the 15th, the Guangdong Provincial Defense General upgraded the windproof emergency response level II to level I. At 17:00 on the 16th, it made landfall in Haiyan Town, Taishan, Guangdong Province. At the time of landfall, the maximum wind speed near the center was 14 on the Beaufort scale, with a minimum central pressure of 955 hPa. By 20:00 on the 17th, the Central Meteorological Station discontinued its numbering due to difficulty in determining its circulation center.

Due to the impact of Super Typhoon Mangkhut, five base towers of a transmission line in a mountainous area of China collapsed. The collapsed tower is located at the transition between the plains and the mountains. In this study, a numerical simulation method is used to calculate the real-time wind speed at the site of the collapsed tower, as actual wind speed data is available from a weather station at the base of the mountain, but there is no weather observation station on the mountain itself.

Numerical simulation refers to the numerical solution of the wind field around an object, often called Computational Fluid Dynamics (CFD), which is conducted on a computer to simulate the actual wind environment [1]. This method is fast, cost-effective, flexible, and intuitive. Addressing the challenges of wind speed assessment in mountainous areas, this study aims to accurately assess wind speeds by constructing high-precision terrain models, integrating multi-source data, optimizing physical models, and enabling cross-scale simulations. This approach provides technical support and a scientific basis for analyzing the impacts of Typhoon Mangkhut.

2. Overview of the incident

The wind incident occurred on a 110 kV line that was put into operation in 1995, and its design followed the "Technical Regulations for Overhead Line Design" (SDJ3-79). The design wind speed for the line, measured at 15 m above ground level with a 15-year return period, was 35 m/s, which corresponds to a wind speed of 32.8 m/s at 10 m above ground [2]. In the affected section between towers N66 and N70, a total of five towers collapsed, all toppling in the same direction, which aligns with the characteristics of high-wind conditions causing tower failure. The topography of the affected tower area is shown in **Figure 1.**

Figure 1. Topographical map of the area of the accidental tower

The main structural material of the five damaged towers, along with the cross-bracing material, experienced varying degrees of destabilization. Specifically, the main structural material at the base of towers N66, N68, and N69 was destabilized, causing the foundations to be uprooted and damaged. In contrast, the middle sections of towers N67 and N70 were destabilized and damaged, while their foundations and ground bolts remained intact. **Table 1** provides the ground level and incident details for each tower, and **Figure 2** and **Figure 3** illustrate the damage to the pole towers.

Table 1. Tower ground elevation and accident situation

Tower number	Elevation of ground (m)	Condition of incident
N66	155	The foundation tilted and the tower collapsed
N67	141	The bending of the tower caused the whole tower to collapse
N68	119	The foundation tilted and the tower collapsed
N69	101	The foundation tilted and the tower collapsed
N70	148	The bending of the tower caused the whole tower to collapse and the ground to crack.

Figure 2. The tower body is bent

Figure 3. The tower foundation gave way

It could be seen from **Figure 1** that towers N66 to N70 were situated along a ridge extending from northwest to southeast. The southwest side of the line was adjacent to a bay, while the northeast side featured the flat terrain of a town. According to data provided by the town's meteorological observation station, the altitude was 26.5 m, with a temperature of 24.8°C during the strong wind period. The relative humidity was 98%, the average pressure was 976.5 hPa, the instantaneous maximum wind speed reached 42.1 m/s, and the average maximum wind speed over 10 min was 31.0 m/s. The average wind direction during the strong wind period was 69°, closely aligning with the vertical orientation of the line. The design wind speed increased significantly due to the elevated terrain. The real-time wind speed at the tower was calculated using the numerical simulation method described below.

3. Numerical simulation of wind speed at tower position

3.1. Model creation and meshing

The SRTM system data published by NASA is used for Digital Elevation Model (DEM) data in the area near the incident tower. Considering the computing power of the workstation and the accuracy of numerical simulation, the DEM data for a 5 km × 5 km area are downloaded, and the boundary is smoothed to form a ground model. The ground model is shown in **Figure 4.** The maximum mountain height in the calculation range is 216 m, and the vertical space of the model is selected to be about 10 times the mountain height. The computational space is meshed using a structured grid, and the grid near the ground is refined.

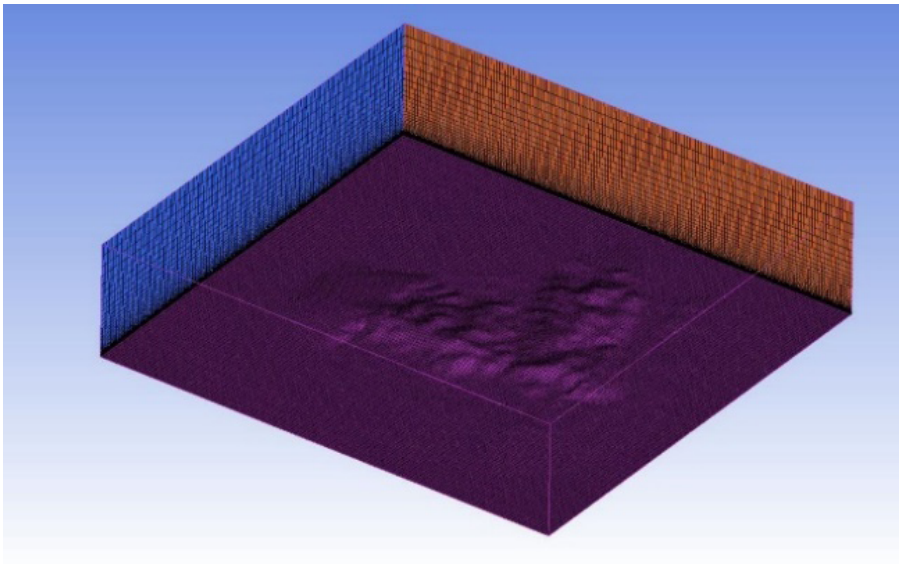

Figure 4. Ground model and meshing within the numerical simulation range

3.2. Setting of boundary conditions

The computation bounds are set considering the following factors. Firstly, the simulated atmospheric flow can be regarded as the flow of incompressible gas. The velocity inlet is selected as the inlet interface, with a wind speed of 31.0 m/s measured by the weather station located below the mountain. Secondly, it is assumed that the gas flow to the outlet has fully developed; thus, the divergence of all physical variables along the outlet is zero, and the pressure outlet is chosen as the outlet interface. Thirdly, the ground is considered to be non-slip, and the wall boundary is selected for the lower interface. Fourthly, it is assumed that at the top of the atmosphere, the vertical velocity is zero and the gradient of all vertical physical variables is zero. Therefore, the symmetry boundary is selected for the upper interface. The selection of the upper interface boundary is particularly important for calculation convergence, as assuming the vertical velocity at this interface to be zero implies that gas is not allowed to enter and exit freely, which is inconsistent with actual conditions. However, it has been observed that achieving calculation convergence becomes difficult when changing several boundaries to better align with real-world conditions [3]. A symmetry boundary is also used on the sides, and the turbulence model employed is the Realizable k-ε model [4].

3.3. Ground roughness treatment

In the near-surface atmospheric boundary layer, the surface roughness, namely the distribution of vegetation, will have a great influence on the vertical distribution of wind speed [5]. The roughness height K_s represents the average height of the roughness elements in the corresponding surface area and is currently one of the main parameters used to characterize roughness conditions [6].

Another parameter describing the surface condition is the roughness length Z_0, which refers to the height from the ground at which the wind speed decreases to zero [7]. The value of the roughness length Z_0 is shown in **Table 2**.

Table 2. Table of values of roughness length Z_0

Surface type	Roughness length, Z_0 (m)	Surface type	Roughness length, Z_0 (m)
Urban, Forest	0.7	Flat meadow	0.01
Suburb	0.3	Snow surface (smooth)	0.001
Countryside, more trees	0.1	Sandy surface (smooth)	0.0003
Open farm, few trees, and buildings	0.03	Water area	0.0001

Table 3. Calculation results of wind speed at different heights of each tower

Ground height/Tower number	N66	N67	N68	N69	N70
10 m	37.2	36.7	35.4	33.0	32.6
20 m	38.3	37.9	36.9	34.6	34.2
30 m	38.9	38.6	37.9	35.8	35.2
40 m	38.8	38.6	38.2	36.6	35.5
50 m	38.3	38.1	37.9	36.6	35.4
60 m	37.7	37.6	37.4	36.4	35.2
70 m	37.2	37.1	37.0	36.1	35.0
80 m	36.8	36.7	36.6	35.9	34.8
90 m	36.5	36.4	36.3	35.7	34.7
100 m	36.2	36.1	36.0	35.5	34.6

Roughness height K_s can be calculated by the following formula:

$$K_s = \frac{2A}{S} Z_0 = \alpha Z_0 \quad (1)$$

In the formula:

A = Calculate the horizontal area of the average single roughness element in the region, m^2;

S = The average cross-sectional area of the windward surface of the ground roughness element,m^2;

α = The conversion factor.

In the atmospheric boundary layer, the roughness length Z_0 is generally about 1/7 to 1/8 of the plant cover height, or approximately equal to 1/10 of the roughness height K_s. In this paper, the value of Z_0 is 0.05, α is 10, and K_s is calculated to be 0.5. The roughness uniformity coefficient C_S indicates the degree of uniformity of ground roughness, which is usually 0.5, and C_S is 0.5 in this paper.

3.4. Results of numerical simulation

The flow field simulation calculation was carried out in the incident tower area, and the wind speed values of towers N66 to N70 at different ground heights were obtained, as shown in **Table 3** and **Figure 5.**

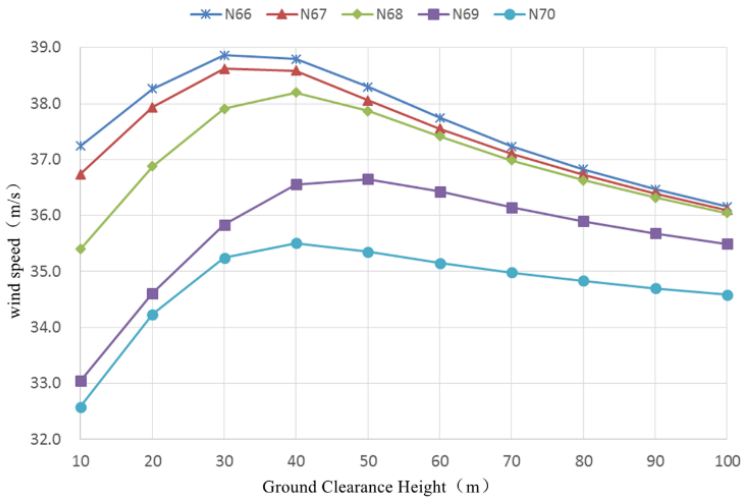

Figure 5. Wind speed values of towers N66 to N70 at different heights above the ground

It can be seen from **Figure 5** that the wind speed at each tower location is greater than the initial wind speed by 31.0 m/s, and the mountain has an obvious acceleration effect on the wind speed. The wind speed at different ground heights increases first and then decreases, and the inflection point appears at the height of 30 m or 40 m above the ground. N66, N67, N68, and N69 four base towers have high wind speed values of 10 m above the ground, which all exceed the design wind speed of 32.8 m/s.

The high wind speed cloud diagram at 10 m above the ground within the scope of the model is shown in **Figure 6**, the high wind speed vector diagram at 10 m above the ground is shown in **Figure 7**, the wind speed cloud diagram at the cross-wind section of tower N66 is shown in **Figure 8**, and the wind speed cloud diagram at the downwind section of tower N66 is shown in **Figure 9.**

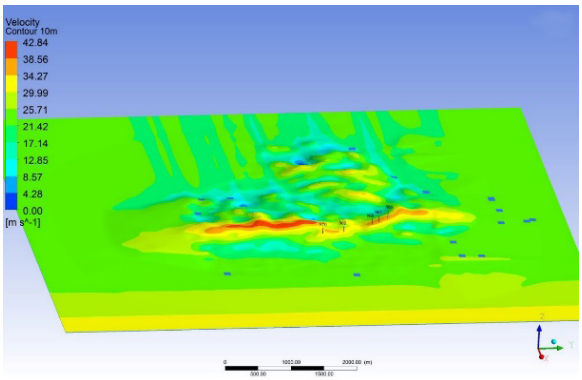

Figure 6. Cloud map of wind speed at 10 m above ground

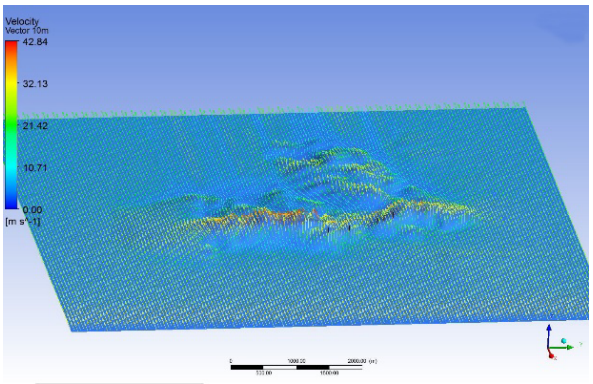

Figure 7. Loss of wind speed at 10 m above ground

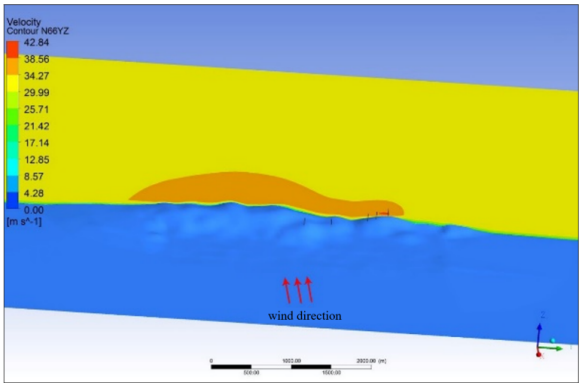

Figure 8. Wind speed cloud map of crosswind section at N66

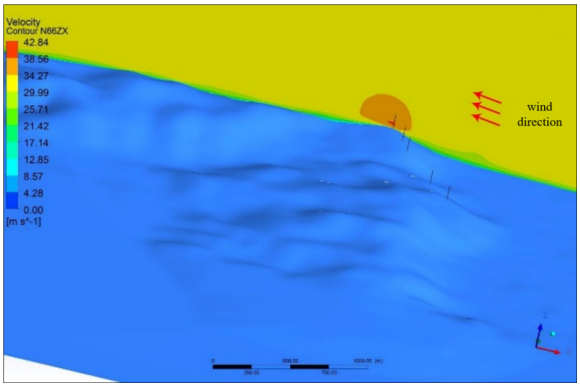

Figure 9. Wind speed cloud map of the downwind section at N66

It can be seen from the above figures that towers N66 to N70 are on the windward slope, thus affected by the mountain acceleration effect. The wind direction at the tower is roughly the same as the initial wind direction, and the local position changes slightly.

4. Conclusion

To analyze the influence of Typhoon Mangkhut on the towers, this paper uses the numerical simulation method to analyze the real-time wind speed value at the tower position. The ground model is established by DEM data of the SRTM system, and the maximum wind speed measured at the meteorological station below the mountain is 31.0 m/s as the boundary condition. The high wind speed at 10 m above ground at N66 is 37.2 m/s, the high wind speed at 10 m above ground at N67 is 36.7 m/s, the high wind speed at 10 m above ground at N68 is 35.4 m/s, the high wind speed at 10 m above ground at N69 is 33.0 m/s, and the wind speed at N66 to N69 is 32.8 m/s higher than the design wind speed. This is one of the main reasons for the wind disaster incident.

Funding

Funded by CRSRI Open Research Program (Project No. CKWV2014202/KY).

Disclosure statement

The authors declare no conflict of interest.

References

[1] Zhao Q, Li R, Cao KF, et al., 2024, Influence of Building Spatial Patterns on Wind Environment and Air Pollution Dispersion Inside an Industrial Park Based on CFD Simulation. Environmental Monitoring and Assessment, 196(5): 427. https://doi.org/10.1007/s10661-024-12593-3

[2] Ministry of Housing and Urban-Rural Development of the People's Republic of China, 2012, Code for Load and Strength of Building Structures: GB 50009-2012. China Architecture & Building Press, Beijing.

[3] Hou X, 2019, Introduction to Power Engineering Structures. China Water & Power Press, Beijing.

[4] Li L, Lijie Z, Ning Z, et al., 2010, Application of FLUENT in the Study of Fine Simulation of Wind Field in Complex Terrain. Plateau Meteorology, 29(3): 621–628.

[5] Kochanski A, Koracin D, Dorman CE, 2006, Comparison of Wind-Stress Algorithms and Their Influence on Wind-Stress Curl Using Buoy Measurements Over the Shelf Off Bodega Bay, California. Deep-Sea Research Part II: Topical Studies in Oceanography, 53(25–26): 2865–2886. https://doi.org/10.1016/j.dsr2.2006.07.008

[6] Deng Y, Liu S, Yu Z, 2010, Influence Analysis of Roughness in CFD Simulation of Actual Terrain Wind Field. Acta Energiae Solaris Sinica, 31(12): 1644–1648.

[7] He FL, Xu Q, Wang N, et al., 2023, Terrain-Influenced Wind Flow of the Qitai Radio Telescope Site. Journal of Mountain Science, 20(11): 3173–3185. https://doi.org/10.1007/s11629-023-8092-8